

Vision-based Aerial Tracking using Intelligent Excitation

Chengyu Cao and Naira Hovakimyan

Abstract—This paper proposes a new technique of intelligent excitation within an adaptive control architecture for aerial tracking using a visual sensor. The adaptive controller is capable of maintaining a relative position for a trailer aircraft with respect to a lead aircraft of unknown size. The only information about the lead aircraft can be deduced from the subtended angle in the image plane of the trailing aircraft. Neither the dimension of the lead aircraft, nor its velocity are assumed to be known to the follower. The control objective of maintaining a prespecified relative range is achieved via an intelligent excitation signal, the properties of which are analyzed in this paper. Simulations illustrate the theoretical results.

I. INTRODUCTION

With the advent of visual sensors, design of intelligent UAVs (unmanned aerial vehicles) that are capable of tracking with the use of *only* visual sensors, has grown into one of the realistic opportunities today. In this paper, we formulate the problem of aerial tracking of two UAVs in the absence of communication channels. The only information that the trailer has about the lead aircraft is the image of the latter from a camera mounted on the head of it. A more or less exhaustive list of publications on this topic, including some innovative algorithms, one can find in [1]–[4] and the references therein. For brevity, we do not elaborate on those here.

The main difference of the problem of visual tracking from standard tracking problems is the way the feedback signal is measured. Visual tracking is done via imaging sensors, which involve a projection of a 3D object onto a 2D plane, consequently rendering the range between the two flying objects unobservable. In addition, we note that the range information has to be extracted via computer vision algorithms before being used in the control loop. Consequently, from the classical control theoretical point of view, one can formulate this as a disturbance rejection/attenuation problem in the presence of highly uncertain time-varying disturbance associated with unpredictable target dynamics. Such view point has been taken in [1]–[4], where Extended Kalman filter and output feedback formulations have been explored to obtain a tracking controller for the trailing aircraft under a certain set of assumptions about the target dynamics. One way

or another, it has been acknowledged that special type of maneuvers are required from the follower to overcome the unobservability aspect of the relative range between the two objects.

In this paper, we are defining a mathematical framework, within which we can characterize the tracking performance of the proposed controller dependent upon the type of maneuvers via an $\epsilon(\delta)$ language. We cast our problem formulation into adaptive control framework, viewing the target size as an unknown constant parameter and the target velocity as an unknown time-varying parameter. The challenge associated with the unobservable relative range is translated into one, having a reference input, dependent upon the unknown constant parameter associated with the target size. We propose a new technique of intelligent excitation and analyze its performance for solving the tracking problem of an unpredictable target. The proposed excitation signal can detect the parameter errors intelligently and initiate an excitation signal only when necessary, as opposed to persistent excitation. At this point we note, that the special maneuvers required in other approaches, like [1]–[4], can be viewed as particular cases of an excitation signal within an adaptive control framework.

Finally, we limit our analysis in this paper to constant (unknown) target velocity and focus on the learning algorithm that leads to relative range recovery. Time variations in the target velocity are discussed in the last section before the simulations. In an alternate paper [7], we present an adaptive disturbance rejection controller for range regulation in the presence of unknown time varying target velocity subject to $\mathcal{L}_\infty \cap \mathcal{L}_2$ constraint in its variation.

The paper is organized as follows. In Section II, we give the problem formulation and develop the state space representation that will be used in the sequel. In Section III, we define the adaptive controller and demonstrate its limitations. In Section IV, we augment the adaptive controller with intelligent excitation and characterize the convergence properties of it in $\epsilon(\delta)$ language. We discuss the case of accelerating target in Section V. Simulation results are provided in Section VI, and Section VII concludes the paper.

II. PROBLEM FORMULATION

Consider the motion of two aircraft in a two-dimensional Cartesian space (X, Y) . Let (x, y) be the vector of relative distance between the two aircraft. In kinematic setting, the relative dynamics can be described

Research supported by AFOSR under MURI subcontract F49620-03-1-0401 and in part under AFOSR grant F49620-03-1-0443.

Chengyu Cao is with Aerospace & Ocean Engineering, Virginia Polytechnic Institute & State University, Blacksburg, VA 24061-0203, e-mail: chengyu@vt.edu, Member IEEE

Naira Hovakimyan is with Aerospace & Ocean Engineering, Virginia Polytechnic Institute & State University, Blacksburg, VA 24061-0203, e-mail: nhovakim@vt.edu, Senior Member IEEE, Corresponding author

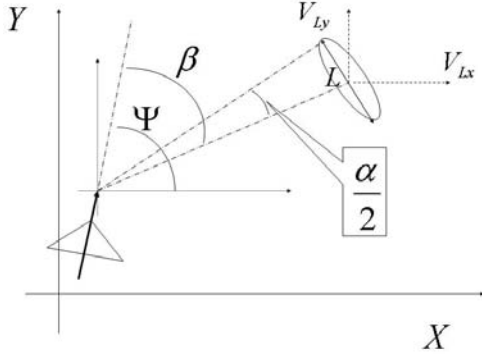


Fig. 1. Bearing and Subtended angles

via the following set of first order differential equations:

$$\dot{x} = u_{lx}(t) - u_{fx}(t), \dot{y} = u_{ly}(t) - u_{fy}(t), \dot{\Psi} = u_{\Psi}(t), \quad (1)$$

where $x, y, \Psi \in \mathbb{R}$, u_{fx} and u_{fy} (u_{lx} and u_{ly}) are the components of the velocity vector of the trailing (lead) aircraft in the X and Y axis respectively, Ψ is the body orientation (yaw) angle of the trailing aircraft and u_{Ψ} is the angular velocity of it. The trailing aircraft has no knowledge of the target or lead aircraft, including u_{lx} , u_{ly} and its characteristic dimension L , except for some conservative upper and lower bounds on u_{lx} , u_{ly} and L , Fig. 1. The vector of the relative position (x, y) is also unknown to the follower, so that the only information about the target position can be deduced from two angles, Fig. 1. The first is called bearing angle

$$\beta = \Psi - \tanh(y/x), \quad (2)$$

while the second is the subtended angle of the target in the image plane

$$\alpha = 2 \tanh(L/(2R)), \quad (3)$$

where R is the range between the two objects:

$$R = \sqrt{x^2 + y^2}. \quad (4)$$

Let $\chi \triangleq (\alpha, \beta, \Psi)$ be the vector of available measurements. With (2)-(4), the coordinates of the relative motion can be expressed as:

$$\begin{aligned} x(\chi) &= \frac{L}{2 \tan(\alpha/2) \sqrt{1 + \tan^2(\Psi - \beta)}} \\ y(\chi) &= \frac{L \tan(\Psi - \beta)}{2 \tan(\alpha/2) \sqrt{1 + \tan^2(\Psi - \beta)}}. \end{aligned} \quad (5)$$

It follows from (1) and (5) that

$$\begin{aligned} \frac{\partial x(\chi)}{\partial \alpha} \dot{\alpha} + \frac{\partial x(\chi)}{\partial \beta} \dot{\beta} + \frac{\partial x(\chi)}{\partial \Psi} \dot{\Psi} &= u_{lx} - u_{fx} \\ \frac{\partial y(\chi)}{\partial \alpha} \dot{\alpha} + \frac{\partial y(\chi)}{\partial \beta} \dot{\beta} + \frac{\partial y(\chi)}{\partial \Psi} \dot{\Psi} &= u_{ly} - u_{fy}. \end{aligned}$$

Thus, the state space model of the relative motion of two aircraft can be written as:

$$\begin{aligned} \begin{bmatrix} \dot{\alpha} \\ \dot{\beta} \end{bmatrix} &= F_a(\chi) \begin{bmatrix} \frac{u_{fx} - u_{lx}}{L} \\ \frac{u_{fy} - u_{ly}}{L} \end{bmatrix} + \begin{bmatrix} 0 \\ 1 \end{bmatrix} u_{\Psi} \\ \dot{\Psi} &= u_{\Psi} \end{aligned} \quad (6)$$

with $\chi(0) = [\alpha_0 \ \beta_0 \ \Psi_0]^\top$, where

$$\begin{aligned} F_a &= \begin{bmatrix} f_{11}(\chi) & f_{12}(\chi) \\ f_{21}(\chi) & f_{22}(\chi) \end{bmatrix} = \frac{2 \tan(\alpha/2) \sin(\alpha)}{\sqrt{1 + \tan^2(\Psi - \beta)}} \\ &\times \begin{bmatrix} 1 & \tan(\Psi(t) - \beta(t)) \\ \frac{-\tan(\Psi(t) - \beta(t))}{\sin(\alpha(t))} & \frac{1}{\sin(\alpha(t))} \end{bmatrix}. \end{aligned} \quad (7)$$

In (6), the control signals are the velocity and angular velocity of the trailing aircraft u_{fx}, u_{fy}, u_{Ψ} . We notice that $0 < \alpha < \frac{\pi}{2}$ from the definition of the subtended angle. In

addition, since $\begin{bmatrix} 1 & \tan(\Psi(t) - \beta(t)) \\ \frac{-\tan(\Psi(t) - \beta(t))}{\sin(\alpha(t))} & \frac{1}{\sin(\alpha(t))} \end{bmatrix}$ has a non-zero determinant and $\frac{2 \tan(\alpha/2) \sin(\alpha)}{\sqrt{1 + \tan^2(\Psi - \beta)}} > 0$, we have

$$\det(F_a(\chi)) \neq 0. \quad (8)$$

Denoting the vector of unknown parameters as

$$\omega(t) \triangleq [\omega_1 \ \omega_2(t) \ \omega_3(t)]^\top = [\frac{1}{L} \ \frac{u_{lx}(t)}{L} \ \frac{u_{ly}(t)}{L}]^\top,$$

we assume that a conservative range for each of these unknown parameters is known

$$\omega_i \in \Omega_i \triangleq [\Omega_{i_{\min}}, \ \Omega_{i_{\max}}], \quad i = 1, 2, 3.$$

We rewrite the system in (6) as:

$$\begin{aligned} \begin{bmatrix} \dot{\alpha} \\ \dot{\beta} \end{bmatrix} &= -F_a \begin{bmatrix} \omega_2 \\ \omega_3 \end{bmatrix} + \omega_1 F_a \begin{bmatrix} u_{fx} \\ u_{fy} \end{bmatrix} + \begin{bmatrix} 0 \\ u_{\Psi} \end{bmatrix} \\ \dot{\Psi} &= u_{\Psi} \quad \chi(0) = \chi_0 = [\alpha_0 \ \beta_0 \ \Psi_0]^\top, \quad t \geq 0. \end{aligned} \quad (9)$$

The control objective is to maintain a prespecified relative position between the two aircraft via the design of u_{fx}, u_{fy}, u_{Ψ} . We will characterize this relative position by three reference signals Ψ_r, β_r and R_r . Ψ_r and β_r are the desired yaw and bearing angles and R_r is the desired range. The main challenge of the *visual* aerial tracking problem has to do with the fact the relative range $R(t)$ is not observable from the measured variables, while it has to be regulated. To this end, we notice that the desired range R_r along with the unknown parameter L uniquely define a desirable subtended angle:

$$\alpha_r = 2 \tanh(L/(2R_r)). \quad (10)$$

So, we will design the control signal to maintain a desired angle α_r , and the range regulation will follow. In addition, we notice that tracking of α_r is challenging due to its dependence upon the unknown parameter L .

III. ADAPTIVE CONTROL FRAMEWORK

We notice that the system in (9) is linearly parameterized in unknown constant and time-varying parameters. The main challenge of having unobservable range $R(t)$ is translated into having a reference signal, dependent upon the unknown length parameter L . This motivates consideration of a reference model, dependent upon the time-varying estimate of the unknown parameter L , as

defined below. For simplicity of presentation of the main analysis tools and for the sake of keeping the development systematic, in this and next section, we assume that the target maintains constant (unknown) velocity. The extension to time-varying velocity of the target is discussed in section V.

A. Adaptive Controller

Define the following reference input:

$$\bar{\alpha}_r(t) = 2 \tanh(1/(2R_r \hat{\omega}_1(t))), \quad (11)$$

where $\hat{\omega}_1(t)$ is the time-varying estimate of the unknown parameter $\omega_1 = 1/L$. Next, consider the following reference model:

$$\begin{bmatrix} \dot{\alpha}_m(t) \\ \dot{\beta}_m(t) \end{bmatrix} = \begin{bmatrix} -k_1(\alpha_m(t) - \bar{\alpha}_r(t)) \\ -k_2(\beta_m(t) - \beta_r) \end{bmatrix}, \quad (12)$$

where $\bar{\alpha}_r(t)$ and β_r are respectively time-varying and constant reference inputs, $k_1 > 0$ and $k_2 > 0$ are design gains. Define the following error signals:

$$\tilde{\alpha}(t) = \alpha_m(t) - \alpha(t), \tilde{\beta}(t) = \beta_m(t) - \beta(t), e = [\tilde{\alpha} \ \tilde{\beta}]^\top.$$

Control signal for the system dynamics in (9) is given as:

$$\begin{bmatrix} u_{fx}(t) \\ u_{fy}(t) \end{bmatrix} = \frac{-F_a^{-1}}{\hat{\omega}_1(t)} \left(F_b + \begin{bmatrix} k_1(\alpha_m(t) - \bar{\alpha}_r(t)) \\ k_2(\beta_m(t) - \beta_r) \end{bmatrix} \right) \\ u_\Psi(t) = -k_3(\Psi(t) - \Psi_r) \quad (13)$$

where $k_3 > 0$ is a proportional design gain to ensure tracking of constant yaw command Ψ_r , $F_b = Ae - F_a[\hat{\omega}_2 \ \hat{\omega}_3]^\top + [0 \ u_\Psi]^\top$, and $a_{11}, a_{12}, a_{21}, a_{22}$ are such that the matrix $A = \begin{bmatrix} a_{11} & a_{12} \\ a_{21} & a_{22} \end{bmatrix}$ is Hurwitz, while $\hat{\omega}_2(t)$ and $\hat{\omega}_3(t)$ are the time-varying estimates of unknown time-varying parameters $\omega_2(t)$ and $\omega_3(t)$. Consider the following adaptive laws, by invoking the projection operator [5]:

$$\begin{aligned} \dot{\hat{\omega}}_1 &= \text{Proj}(\hat{\omega}_1(t), -\frac{1}{k_{v1}} e(t)^\top P F_a [u_{fx} \ u_{fy}]^\top) \\ \dot{\hat{\omega}}_2 &= \text{Proj}(\hat{\omega}_2(t), \frac{1}{k_{v2}} e(t)^\top P F_a [1 \ 0]^\top) \\ \dot{\hat{\omega}}_3 &= \text{Proj}(\hat{\omega}_3(t), -\frac{1}{k_{v3}} e(t)^\top P F_a [0 \ 1]^\top) \\ \text{Proj}(\hat{\omega}_i(t), x) &= \begin{cases} x & \hat{\omega}_i(t) \in (\Omega_{i_{\min}}, \Omega_{i_{\max}}) \\ 0 & \hat{\omega}_i(t) \geq \Omega_{i_{\max}}, x > 0 \\ 0 & \hat{\omega}_i(t) \leq \Omega_{i_{\min}}, x < 0 \end{cases} \\ \hat{\omega}(0) &= \hat{\omega}_0, \quad t \geq 0, \end{aligned} \quad (14)$$

where k_{v1}, k_{v2} , and k_{v3} are positive design gains, $\hat{\omega}(t) \triangleq [\hat{\omega}_1(t) \ \hat{\omega}_2(t) \ \hat{\omega}_3(t)]$, and $P = P^\top > 0$ solves the Lyapunov equation: $A^\top P + PA = -Q$ for arbitrary $Q > 0$. Thus, the complete adaptive controller is defined via (11), (12), (13) (14). With control signal in (13), the closed-loop dynamics of the state variable Ψ is decoupled from the whole system and can be written as:

$$\dot{\Psi}(t) = -k_3(\Psi(t) - \Psi_r). \quad (15)$$

Remark 1: We note that in case if the characteristic dimension L of the target size is known, then (10) defines

uniquely the reference input α_r . This in turn alleviates the need for the estimation of ω_1 . The resulting adaptive controller is then similar to the classical linear in parameters adaptive controller [6].

Remark 2: We note that in steady state a desirable yaw command is $\tan(\Psi_r) = \frac{u_{fy}}{u_{fx}}$. For simplicity, however, in this paper the yaw command Ψ_r generation is assumed to be independent of the follower's velocity.

B. Properties of the Adaptive Controller

We notice from (13) that

$$[-k_1(\alpha_m - \bar{\alpha}_r) - k_2(\beta_m - \beta_r)]^\top = \hat{\omega}_1 F_a [u_{fx} \ u_{fy}]^\top + F_b.$$

This leads to the following form of the tracking error dynamics between the system in (9) and reference model in (12):

$$\dot{e} = Ae(t) - F_a(\chi)[\tilde{\omega}_2 \ \tilde{\omega}_3]^\top + \tilde{\omega}_1 F_a(\chi)[u_{fx} \ u_{fy}]^\top \quad (16)$$

where $\tilde{\omega}_i = \hat{\omega}_i - \omega$, $i = 1, 2, 3$. The following lemma proves that the tracking error dynamics are asymptotically stable. All the proofs of the Lemmas and Theorems in this paper can be found in [8].

Lemma 1: For the system in (9), the adaptive controller in (11), (12), (13), (14) ensures that $\lim_{t \rightarrow \infty} e(t) = 0$.

We recall that the control objective is to ensure that $\beta(t) \rightarrow \beta_r$, $\Psi(t) \rightarrow \Psi_r$ and $R(t) \rightarrow R_r$ as $t \rightarrow \infty$. The next lemma proves that for constant reference inputs the adaptive controller defined via (11), (12), (13) and (14) achieves asymptotic tracking for *part* of these variables.

Lemma 2: For the system in (9) and constant reference signals β_r , Ψ_r and R_r , the adaptive controller defined via (11), (12), (13) and (14) ensures that

$$\lim_{t \rightarrow \infty} \beta(t) = \beta_r \quad \lim_{t \rightarrow \infty} \Psi(t) = \Psi_r. \quad (17)$$

Here we notice that the adaptive controller does not ensure that $\lim_{t \rightarrow \infty} \hat{\omega}_1(t) = \omega_1$, despite the fact that $\tilde{\omega}(t)$ is bounded. Since this bound cannot be quantified, we cannot characterize the convergence of $\bar{\alpha}_r(t)$ or $\alpha(t)$ to α_r . Therefore, one of the control objectives

$$\lim_{t \rightarrow \infty} R(t) \rightarrow R_r \quad (18)$$

is not met. In the next section we propose an intelligent excitation signal for overcoming this deficiency.

IV. ADAPTIVE CONTROLLER WITH INTELLIGENT EXCITATION

To achieve (18), we propose the following modification of $\bar{\alpha}_r$ in the definition of (11):

$$\bar{\alpha}_r(t) = 2 \tanh(1/(R \hat{\omega}_1(t))) + E_x(t), \quad t \geq 0 \quad (19)$$

where $E_x(t)$ is the signal of intelligent excitation, defined as: $E_x(t) = k_x(t) \sin(k_{x5} t)$, where $k_{x5} > 0$ is a design gain. The objective in this section is to define $k_x(t)$ in a way to ensure that $E_x(t)$ vanishes when the norm of the

parameter error $\tilde{\omega}(t)$ is less than an a priori prespecified desirable design characteristic.

For adaptive controller with intelligent excitation, it can be checked easily that Lemmas 1 and 2 hold, since the proofs did not rely on the particular definition of $\alpha_r(t)$. Next we show that the adaptive controller (12), (13), (14) with intelligent excitation (19) will achieve the desired range tracking objective. To this end, denote $\Xi \triangleq [\alpha \ \beta \ \Psi \ \alpha_m \ \beta_m \ \hat{\omega}_1 \ \hat{\omega}_2 \ \hat{\omega}_3]^\top$, and write the dynamics for it:

$$\dot{\Xi}(t) = \begin{cases} (f_{11}u_{fx} + f_{12}u_{fy})\omega_1 - f_{11}\omega_2(t) - f_{12}\omega_3(t) \\ (f_{21}u_{fx} + f_{22}u_{fy})\omega_1 - f_{21}\omega_2(t) - f_{22}\omega_3(t) + u_\Psi \\ -k_1(\alpha_m(t) - \bar{\alpha}_r(t)) \\ -k_2(\beta_m(t) - \beta_r) \\ \text{Proj}\left(\hat{\omega}_1, -\frac{1}{k_{v1}}e^\top PF_a[u_{fx} \ u_{fy}]^\top\right) \\ \text{Proj}\left(\hat{\omega}_2, \frac{1}{k_{v2}}e^\top PF_a[1 \ 0]^\top\right) \\ \text{Proj}\left(\hat{\omega}_3, \frac{1}{k_{v3}}e^\top PF_a[0 \ 1]^\top\right) \end{cases}$$

$$\Xi(0) = \Xi_0 = [\alpha_0 \ \beta_0 \ \Psi_0 \ \alpha_{m0} \ \beta_{m0} \ \hat{\omega}_0^\top]^\top, \quad (20)$$

where β_r, Ψ_r, R_r are constant reference inputs, and $\bar{\alpha}_r$ is defined in (19). With finite Ξ_0 , it follows from Lemma 1 and eq. (15) that $\Xi(t)$ belongs to a compact set Ξ_c , $\forall t \geq 0$. We notice that the right hand side of system (20) is defined via bounded signals, therefore the solution $\Xi(t)$ is Lipschitz continuous in time t .

To complete the definition of the intelligent excitation signal in (19), one needs to specify an algorithm for designing $k_x(t)$. We recall that in Lemma 1 we have proven that the derivative of the Lyapunov function was negative semidefinite. Next we show that if $k_x(t) = c > 0$ is a constant, then $\dot{V}(t)$ is a negative definite function. To this end, recall that $\dot{V}(t) \leq -e^\top(t)Qe(t) \leq 0$, so that the magnitude of $e^\top(t)Qe(t)$ can be used to analyze the rate of decrease of $V(t)$. Further, let $k_{x2} = \frac{2\pi}{k_{x5}}$ be the period of $E_x(t)$. For any time instant $t_c \in [0, \infty)$, consider the set of the state vectors $\Xi(t_c)$ within Ξ_c , for which the level set of the Lyapunov function takes a prespecified value $V(t_c) = v$. Consider the map $g : [0, \infty) \times [0, \infty) \rightarrow [0, \infty)$:

$$g(v, c) = \min_{\Xi(t_c) \in \Xi_c, t_c \in [0, \infty)} \int_{\tau=t_c}^{t_c+k_{x2}} e^\top(\tau)Qe(\tau)d\tau. \quad (21)$$

Since the input $E_x(t)$ to the reference signal (19) is a periodic function with period k_{x2} , the minimization over a semiinfinite time-interval $t_c \in [0, \infty)$ is equivalent to minimization over a finite time-interval $t \in [0, k_{x2}]$:

$$g(v, c) = \min_{\Xi(t_c) \in \Xi_c, t \in [0, k_{x2}]} \int_{\tau=t}^{t+k_{x2}} e^\top(\tau)Qe(\tau)d\tau.$$

It follows directly that for all (v, c) we have $g(v, c) \geq 0$. First, we note that $g(v, c)$ is independent of t_c and just depends on v and c . Secondly, it can be verified that g is a continuous function of its arguments since $\int_{t=t_c}^{t_c+k_{x2}} e^\top(\tau)Qe(\tau)d\tau$ is continuously depending upon

initial conditions $\Xi(t_c) \in \Xi_c$. Next we prove that $g(v, c)$ can be 0 only at the origin.

Lemma 3: The following statements are true:

- If $v = 0$, then $g(v, c) = 0$.
- If $c > 0$ and $g(v, c) = 0$, then $v = 0$.

Thus, for constant nonzero $k_x(t) = c$ we have $\dot{V} < 0$. Next we need to derive an expression for $k_x(t)$ in a way that it vanishes as $V(t) < v$, where $v > 0$ is a design constant a priori prespecified by us. And this will complete our definition of intelligent excitation.

Let k_{x3} be the maximum allowable value for the excitation amplitude k_x , specified by design constraints. Then, choose $\epsilon > 0$, and define the following map $\bar{g} : [0, \infty) \times [0, k_{x2}] \rightarrow [0, \infty)$ such that

$$\bar{g}(v, \epsilon) = \min_{c \in [\epsilon, k_{x3}], \bar{v} \in [v, V(0)]} g(\bar{v}, c). \quad (22)$$

Since $g(v, c)$ is continuous for all $c \in [\epsilon, k_{x3}]$ and $\bar{v} \in [v, V(0)]$, it follows that \bar{g} is also a continuous function of its arguments. Next we prove that $\bar{g}(v, \epsilon)$ has the same properties as $g(v, c)$.

Lemma 4: If $v = 0$, then $\bar{g}(v, \epsilon) = 0$. The opposite is true only for positive ϵ , i.e. if $\bar{g}(v, \epsilon) = 0, \epsilon > 0$, then $v = 0$.

Corollary 1: For any $\epsilon > 0$ and $v > 0$, there exists a neighborhood $[0, \delta(v, \epsilon)]$ of the origin such that

$$\begin{aligned} \bar{g}(\bar{v}, \epsilon) &\leq \bar{g}(\delta(v, \epsilon), \epsilon) \leq \bar{g}(v, \epsilon), \quad \bar{v} \in [0, \delta(v, \epsilon)] \\ \bar{g}(\bar{v}, \epsilon) &> \bar{g}(\delta(v, \epsilon), \epsilon), \quad \bar{v} > \delta(v, \epsilon). \end{aligned} \quad (23)$$

The proof follows from the definition of $\bar{g}(v, \epsilon)$ in (22) and Lemma 4. The definition in (22) implies that $\bar{g}(\bar{v}, \epsilon)$ is a nonnegative function, while Lemma 4 ensures that it is a positive definite function of $\epsilon > 0$. Hence, for every fixed $\epsilon > 0$, there exists a neighborhood $[0, \delta(v, \epsilon)]$, such that (23) and (24) hold.

Next we define the excitation amplitude as a function of the tracking error signal $e(t)$:

$$k_x(t) = \begin{cases} k_{x3}, & t \in [0, k_{x2}) \\ \min\{k_{x1} \int_{t-k_{x2}}^t e(\tau)^\top Qe(\tau)d\tau, k_{x3} - k_{x4}\} + k_{x4}, & t \in [k_{x2}, \infty) \end{cases} \quad (25)$$

$$k_{x4} = \epsilon, \quad k_{x1} \geq (k_{x3} - k_{x4})/\bar{g}(\delta(v, \epsilon), \epsilon), \quad (26)$$

$\epsilon \in [0, k_{x3})$ and $v \geq 0$ are arbitrary design constants. The next lemma characterizes the decrease rate of the Lyapunov function in finite time for the excitation amplitude defined in (25).

Lemma 5: For arbitrary $v > 0$ such that $V(0) \geq v$, let $[0, T]$ be the time interval for which $V(T) \geq v$ and $V(t) < v$ when $t \in (T, \infty)$. Then the adaptive controller in (12), (13), (14), (19) ensures that

$$k_x(t) = k_{x3}, \quad t \in [0, k_{x2} + T].$$

Moreover, T is finite.

Finally, we have the following lemma.

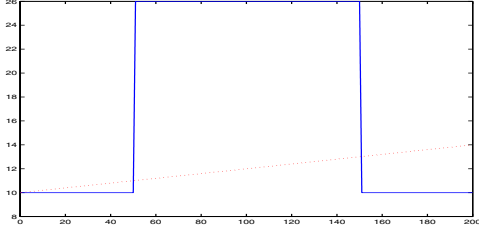


Fig. 2. Trajectories of $u_{lx}(t)$ for rapid change (solid) and gradual varying (dotted) scenarios.

Lemma 6: For the system in (9) with constant reference signals β_r , Ψ_r and R_r , the adaptive controller in (12), (13), (14), (19), guarantees the following convergence bound for the relative range $R(t)$ as $t \rightarrow \infty$:

$$|R(t) - R_r| \leq \max_{|z| \leq \gamma(v, \epsilon)} \left| \frac{L}{2 \tanh(\frac{\alpha r}{2} + z)} - \frac{L}{2 \tanh(\frac{\alpha r}{2})} \right| \quad (27)$$

$$\gamma(v, \epsilon) = \max_{\bar{\omega}_1 \in \left[\omega_1 - \sqrt{\frac{v}{k_{v1}}}, \omega_1 + \sqrt{\frac{v}{k_{v1}}} \right]} (\epsilon + 2 \left| \tanh\left(\frac{1}{R_r \bar{\omega}_1}\right) - \tanh\left(\frac{1}{R_r \omega_1}\right) \right|). \quad (28)$$

Theorem 1: For the system in (9) with constant reference signals β_r , Ψ_r and R_r , the adaptive controller with intelligent excitation in (12), (13) ensures that $\lim_{\epsilon \rightarrow 0, v \rightarrow 0} (\lim_{t \rightarrow \infty} R(t)) = R_r$.

The following remarks discuss the practical implementation issues.

Remark 3: For practical implementation, due to the presence of constant noise and transient tracking error, we can choose $k_{x_4} = 0$ without worrying about the premature disappearance of the intelligent excitation. The value of k_{x_1} should be big enough to guarantee the desired precision. There is no need to characterize the maps g and δ explicitly as in the analysis above.

Remark 4: It follows from Lemma 5 that we can use $k_x(t)$, the amplitude of the excitation signal, to check the parameter convergence. Given a criteria for parameter convergence specified via $\eta \in [k_{x_4}, k_{x_3})$, if for some t' such that $k_x(t) \leq \eta, \forall t \in [t', t' + k_{x_2}]$, we can store the parameter estimates and use it afterwards:

$$\begin{aligned} \bar{\alpha}_r(t) &= 2 \tanh(1/(R_r \bar{\omega}_1)), & t \geq t' + k_{x_2} \\ \bar{\omega}_1 &= \hat{\omega}_1(t' + k_{x_2}), \end{aligned} \quad (29)$$

from where it is obvious that bigger k_{x_1} and smaller η lead to smaller v . The bound for $R(t) - R_r$, as $t \rightarrow \infty$, is defined in (27).

V. TIME-VARYING PARAMETERS

In section III and IV, we assumed that the velocity of the leader aircraft is an unknown constant. In this section, we will address the situation where $u_{lx}(t)$ and $u_{ly}(t)$ are time-varying unknown parameters. The idea is to make the convergence rate of the adaptive controller faster than the change rate of $\omega_2(t)$ and $\omega_3(t)$.

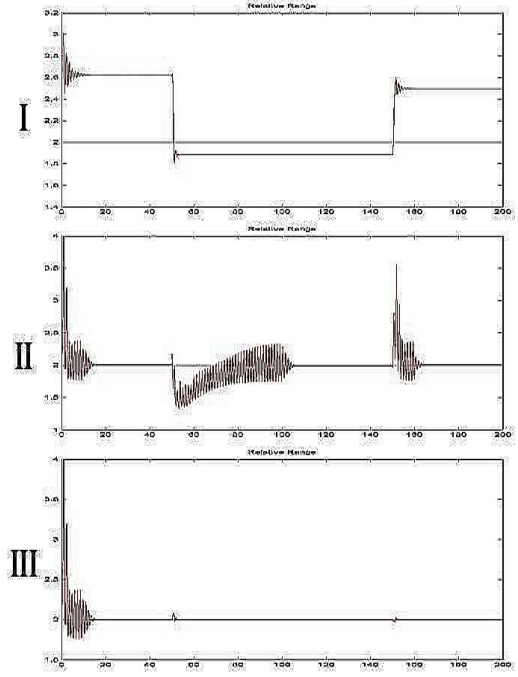


Fig. 3. Trajectory of $R(t)$ with controllers (I), (II) and (III)

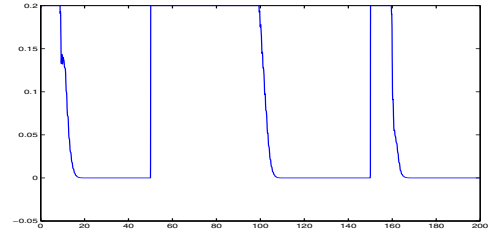


Fig. 4. Trajectory of $k_x(t)$ with controller (II)

Since the change rate of $\omega_2(t)$ and $\omega_3(t)$ are out of our control, we can assume that in the worst scenario they will increase the value of the Lyapunov function. We set the design parameters to make the decreasing rate of Lyapunov function due to parameter error faster than the increase rate due to uncontrolled parameter variation. In what follows, we will give an analysis of the effects of the design parameters on the convergence of the adaptive controller and it will be helpful in the design of the adaptive controller with intelligent excitation for the time-varying velocity of the lead aircraft.

We will use the change in $u_{lx}(t)$ to illustrate the effects. Same results apply to $u_{ly}(t)$. In the Lyapunov function, we note that unknown parameter change will cause an increase of $V(t)$, the increase rate being proportional to design parameters k_{v2} . Every time when $\tilde{\omega}(t)$ leaves the origin, the intelligent excitation takes effect, i.e. $E_x(t) = k_{x_3} \sin(k_{x_5} t)$. The excitation will generate tracking error and consequently reduce $V(t)$, as stated in Lemma 3.

The tracking error is generally bigger with bigger k_{x_3} . However, since k_{x_3} will cause transient error in $R(t) - R_r$ directly, we do not want to choose k_{x_3} sufficiently large. For the same tracking error, the decreasing rate in V increases proportional to the smallest eigenvalue of Q . Therefore with Q , having bigger eigenvalues, and choosing smaller k_{v_2} , the parameter convergence rate can be made faster than the divergence due to unknown parameter variation. The tradeoff here is that we need faster computation and control signals to obtain fast convergence rate of the adaptive controller. Rigorous analysis of this case will be provided in a forthcoming publication.

VI. SIMULATION RESULTS

In this Section, we provide simulation results for the set of reference inputs: $\beta_r = 1$, $\Psi_r = 0$, $R_r = 2$ for the system in (9). Since the tracking performance of $\Psi(t)$ and $\beta(t)$ is not related to the intelligent excitation and is the same as in classical adaptive control frameworks, we will focus only on the tracking performance of $R(t)$ within this section. As we said, this is equivalent to the tracking performance of $\alpha(t)$. Since the changes in leader velocity components u_{lx} and u_{ly} are symmetric within this problem, we set $u_{ly}(t) = 10$, $t \geq 0$, and consider the change in $u_{lx}(t)$ to demonstrate the tracking performance under unknown leader acceleration. We provide simulation results for two different scenarios. One is that $u_{lx}(t)$ experiences a rapid change from one constant value to another and holds there. Another is that $u_{lx}(t)$ changes gradually. These two profiles are plotted in Fig. 2. For rapidly changing $u_{lx}(t)$, we implement three different adaptive controllers and compare them.

(I.) The adaptive controller without intelligent excitation as in (11), (12), (13), (14), is implemented with the following parameters: $A = \begin{bmatrix} -2 & 0 \\ 0 & -2 \end{bmatrix}$, $P = \begin{bmatrix} 5 & 0 \\ 0 & 5 \end{bmatrix}$, $k_{v_1} = 5$, $k_{v_2} = 0.01$, $k_{v_3} = 0.01$, $k_1 = 15$, $k_2 = 15$, $k_3 = 15$.

(II.) The adaptive controller with intelligent excitation as in (12), (13), (14), (19), is implemented with the same parameters as before along with the following parameters for intelligent excitation: $k_{x_1} = 2000$, $k_{x_2} = 2\pi/5$, $k_{x_3} = 0.2$, $k_{x_4} = 0$, $k_{x_5} = 5$.

(III.) The adaptive controller with intelligent excitation as in (12), (13), (14), (19) is implemented, and, after the transient, the parameter estimates are stored and further used in the adaptive controller without excitation (29). All the parameters are as above, and in addition the error tolerance for the estimation is set to $\eta = 0.0005$.

The tracking performance of $R(t)$ with the three different controllers is plotted in Fig. 3. It is shown that $R(t)$ does not converge to R_r with controller (I). The trajectory of $k_x(t)$ of controller (II), which defines the magnitude of excitation signal, is plotted in Fig. 4. The figures demonstrate that every time when parameter error occurs,

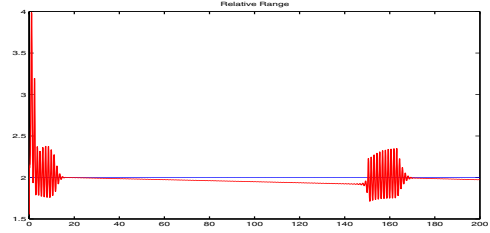


Fig. 5. Trajectory of relative range $R(t)$ with controller (II)

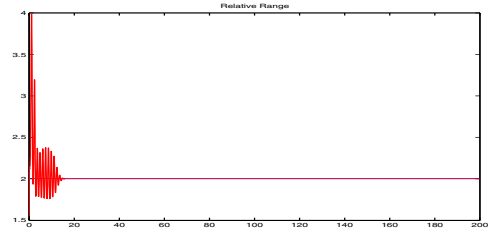


Fig. 6. Trajectory of relative range $R(t)$ with controller (III)

the excitation is initiated with the maximum magnitude $k_x(t) = k_{x_3}$. As $V(t)$ converges to a neighborhood of zero, $k_x(t)$ reduces automatically. If the unknown parameter changes, the excitation is automatically initiated.

For slowly changing $u_{lx}(t)$, the tracking performance of $R(t)$ with the controller of type (II) is plotted in Fig. 5. It can be seen that excitation is initiated when the change in unknown leader velocity drives the parameter error outside the prespecified bound. Fig.6 shows the tracking performance of controller type (III).

VII. CONCLUSION

An adaptive controller with intelligent excitation for vision-based aerial tracking is developed and its ability to regulate the relative range, which is not observable from the measured variables, is demonstrated.

REFERENCES

- [1] Amir Betser, Patricio Vela, and Allen Tannenbaum Automatic Tracking of Flying Vehicles Using Geodesic Snakes and Kalman Filtering, *43rd Conference on Decision and Control*, 2004.
- [2] Y. Watanabe, E.N. Johnson and A. J. Calise Optimal 3-D Guidance from a 2-D Vision Sensor. *AIAA GNC Conf. and Exh.*, 2004.
- [3] E.N. Johnson, A.J. Calise, R. Sattigeri, and Y. Watanabe Approaches to Vision-Based Formation Control. *AIAA GNC Conf. and Exh.*, 2004.
- [4] R. Sattigeri, A.J. Calise, and J.H. Evers An adaptive approach to vision-based formation control. *AIAA GNC Conf. and Exh.*, 2003.
- [5] J.B. Pomet and L. Praly Adaptive Nonlinear Regulation: Estimation from the Lyapunov Equation. *IEEE Trans. Autom. Contr.*, 37(6):729-740, 1992.
- [6] K. S. Narendra, A.M. Annaswamy Stable Adaptive Control. Prentice Hall, 1989.
- [7] V. Stepanyan and N. Hovakimyan An Adaptive Disturbance Rejection Controller for Visual Tracking of a Maneuvering Target Accepted by *AIAA GNC Conf. and Exh.*, 2005.
- [8] C. Cao and N. Hovakimyan Vision Based Aerial Tracking Using Intelligent Excitation. Submitted to *Automatica*.